

See discussions, stats, and author profiles for this publication at: <https://www.researchgate.net/publication/7396639>

Redox Properties of Self-Assembled Gold Nanoclusters

ARTICLE *in* THE JOURNAL OF PHYSICAL CHEMISTRY B · JANUARY 2006

Impact Factor: 3.3 · DOI: 10.1021/jp055229l · Source: PubMed

CITATIONS

21

READS

35

2 AUTHORS:



Bin Su

Zhejiang University

81 PUBLICATIONS 1,111 CITATIONS

SEE PROFILE



Hubert H Girault

École Polytechnique Fédérale de Lausanne

556 PUBLICATIONS 13,985 CITATIONS

SEE PROFILE

Redox Properties of Self-Assembled Gold Nanoclusters

Bin Su and Hubert H. Girault*

Laboratoire d'Electrochimie Physique et Analytique, Ecole Polytechnique Fédérale de Lausanne, Station 6, CH-1015 Lausanne, Switzerland

Received: September 15, 2005; In Final Form: October 11, 2005

The redox properties of a monolayer of alkanethiolate-protected gold nanoclusters (MPCs) constructed on a gold slide electrode was studied in 1,2-dichloroethane (DCE) electrolyte solutions. The influence of the electrostatic interaction between attached MPCs and the substrate electrode on the absolute standard redox potential of MPCs was theoretically considered and studied experimentally.

1. Introduction

The electrochemistry of alkanethiolate-protected gold nanoclusters (MPCs) (prepared by the Brust's reaction^{1,2}) has been extensively studied in the past few years.^{3–9} At room temperatures, successive single electron-transfer events are observed for MPCs in the form of a series of evenly spaced current peaks on the potential axis in voltammetries. The thermodynamics of these successive electron-transfer reactions was first outlined by Chen et al.,⁵ who ascribed the occurrence of the successive electron transfer to quantized charging of the extremely small (sub-atto-Farad, aF) molecular capacitance (C_{MPC}) of the MPC associated with a combination of a small metallic core and a dielectric protecting layer. Then the formal potentials of the charging reactions were formulated with respect to the potential of zero charge of the MPC (E_{PZC}). In terms of this model, the determination of the charge state of the MPC largely depends on the measurement of E_{PZC} , which is, however, difficult to measure experimentally. Additionally, it should be pointed out that the effect of the solvent dielectric was also neglected in this model.

Indeed, the electrochemical properties of MPCs in electrolyte solutions were found to be dependent upon a variety of factors, including the monolayer thickness and dielectric property,¹⁰ the temperature,¹¹ as well as the solvent and the supporting electrolyte in it.^{7,10,12} More recently, by considering an MPC as a “giant molecule” and electron transfers as classical electrochemical reactions, the absolute standard redox potential of freely diffusing MPCs in electrolyte solutions has been theoretically formulated by taking the solvent effect into account and verified experimentally.¹³ According to this formulism, the valence state of MPCs at a given potential can be estimated by employing an internal redox molecular reference, such as ferrocenium/ferrocene.

MPCs demonstrate redox properties, not only in the electrolyte solutions, but also on the solid electrodes as monolayers or multilayers.^{14–17} Freely diffusing MPCs undergo quite fast electron-transfer reactions among MPC cores, and the equilibrium of the MPCs solution can be described in terms of the Nernst equation.¹⁸ Comparatively, the electron-transfer reactions between electrodes and surface-attached MPCs have been reported to occur very slowly in a range of 10–200 s^{−1}.^{14–16,19}

On the other hand, the successive redox reactions of the MPCs, which are anchored onto a gold electrode surface through the dithiol linkers, occur with a smaller potential separation as compared to those of freely diffusing MPCs in solutions.¹⁶ In the present paper, this observation is theoretically considered by taking the electrostatic interaction between anchored MPCs and the substrate electrode into account, which can be formulated in terms of the classical electrostatic model of image charges. The formulation is verified experimentally by studying the electrochemical responses of the MPC monolayer assemblies in 1,2-dichloroethane (DCE) electrolyte solutions.

2. Experimental Section

2.1. Preparation of Gold Slide Electrodes. The gold slide electrodes were prepared as follows: microscopic glass slides (1-mm-thick) were cut into the desired size as the substrates for deposition of gold thin film. The glass substrates were first sonicated separately in acetone, ethanol, and ultrapure water for 20 min each and then immersed in the Piranha solution, a 4:1 mixture of concentrated sulfuric acid (H₂SO₄) and hydrogen peroxide (30% H₂O₂ in water) for 1 h. After that, the glass substrates were rinsed with water and dried under a stream of argon gas. The clean glass slides were then fixed on an aluminum mask to evaporate a thin gold film of the required area of 0.9 cm². The evaporation was carried out in an Edwards Auto 306 evaporator operating at a pressure of less than 5 × 10^{−6} mbar. The evaporation procedure is as follows: a 1-nm-thick chromium (99.99%, Balzer) buffer layer was initially deposited on the glass slide at a deposition rate of 0.1 nm s^{−1} to improve adhesion of the gold film. Then, 100 nm of gold (99.99%, Balzer) film was evaporated on the glass slide, the first 5 nm of which was deposited at a rate of 0.1 nm s^{−1} and the rest at 0.5 nm s^{−1}.

2.2. Fabrication of MPC Assemblies. The gold nanoparticles protected by 1-hexanethiol (called C₆Au MPCs in this work) with a mean diameter of 1.6 ± 0.4 nm in the metallic core were prepared as previously described.¹³ The protocol of assembling Au MPCs onto a gold slide electrode surface was the same as previously described, involving two steps: surface ligand exchange and self-assembling.¹⁵ Briefly, the prepared C₆Au MPCs were first submitted to a ligand exchange reaction with 1,9-nonanedithiol. In a typical reaction, 60 mg of C₆Au MPCs and 4 μL 1,9-nonanedithiol were co-dissolved in 10 mL of

* Corresponding author. E-mail: hubert.girault@epfl.ch. Telephone: +41-21 693 3151. Fax: +41-21 693 3667.

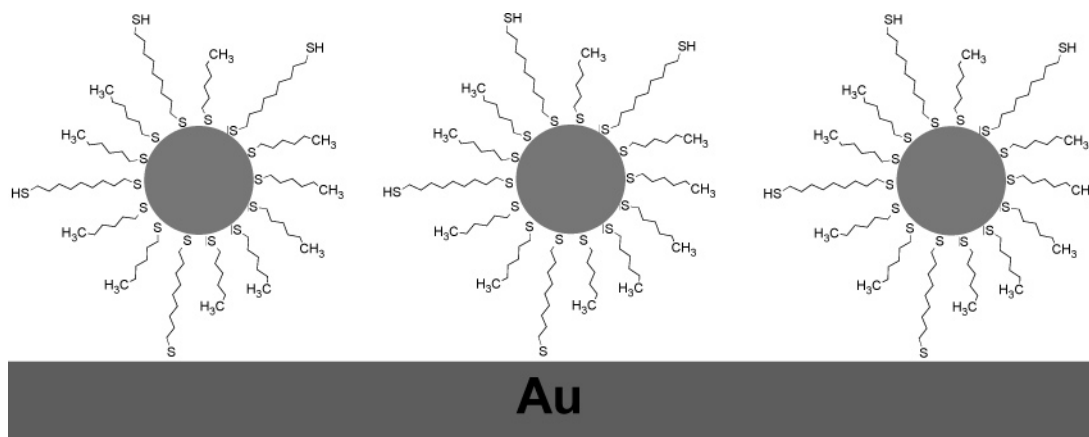


Figure 1. Schematic illustration of the self-assembly of (C₆–C₉)Au MPCs on the gold slide electrode surface.

hexane in a round-bottom flask, and the mixture was stirred for about 36 h. During this period, some ligands on the particle surface were displaced by 1,9-nonanedithiol. Some precipitates were also found to stick on the flask wall due to the intercalation and cross-linking by the 1,9-nonanedithiol. The hexane solution was treated by repeated extraction with absolute ethanol to remove excessive and displaced thiol ligands. Then the resulting solution contained Au MPCs protected by a mixed monolayer of 1-hexanethiol and 1,9-nonanedithiol, called (C₆–C₉)Au MPCs, where the free thiol groups of 1,9-nonanedithiol on the surface of the MPC sphere serve as anchor sites for MPC self-assembling on the gold electrode. The self-assembling of (C₆–C₉)Au MPCs on the Au slide electrode was simply performed by immersing the Au slide electrode into the above-mentioned hexane solution for, typically, 36 h. The electrode was then rinsed with copious amounts of hexane to remove loosely bound MPCs and dried in an argon stream. Figure 1 shows the architecture of an MPC assembly, in which a monolayer of (C₆–C₉)Au MPCs is believed to be constructed on the gold electrode surface.¹⁵

2.3. Electrochemical Measurements. Cyclic voltammetry (CV) and differential pulse voltammetry (DPV) were carried out on a CHI-900 electrochemical workstation (CH-Instruments, TX). CV and DPV measurements of freely diffusing C₆Au MPCs in 1,2-dichloroethane (DCE) electrolyte solutions were carried out in a two-electrode arrangement, in which a 25- μ m-diameter disk-shaped Pt microelectrode (CH-Instruments, TX) was used as the working electrode, and a silver wire was used both as a quasi-reference electrode (QRE) and counter electrode. The potential was corrected to the ferrocenium/ferrocene (Fc⁺/Fc) by adding Fc to the cell at the end of the measurement. Electrochemical measurements of (C₆–C₉)Au MPC assemblies were performed in a three-electrode cell, in which a gold slide electrode functions as the working electrode (WE) and a platinum wire and a silver wire as the counter electrode (CE) and quasi-reference electrode (QRE), respectively. The parameters for DPV measurements in all cases were selected as follows: scan rate 10 mV s⁻¹, pulse height 50 mV, pulse width 60 ms, and period 200 ms.

3. Results and Discussions

The successive single-electron-transfer property of freely diffusing MPCs was first studied in the organic electrolyte solutions for comparison. Figure 2a shows the DPV responses of C₆Au MPCs in DCE with 0.05 M tetra-*n*-butylammonium perchlorate (TBAClO₄) as the supporting electrolyte. A series of well-resolved current peaks are spaced approximately the

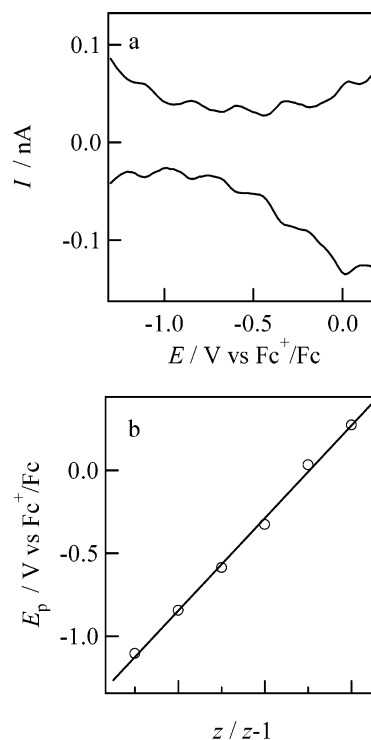


Figure 2. (a) DPV responses of freely diffusing C₆Au MPCs in DCE with 0.05 M TBAClO₄ as supporting electrolyte; (b) linear relation between the peak potentials in (a) and the charge state of MPCs.

same distance apart on the potential axis. They are related to the serial changes of the MPC core charge by successive single-electron transfers. In this sense, MPCs can be treated as multivalent redox species. The absolute standard redox potential of a redox electrochemical reaction associated with MPCs can be derived from a thermodynamic cycle.¹³ For the freely diffusing MPCs in solutions, it is:

$$[E_{Z/Z-1}^0]_{\text{abs,bulk}} = \frac{\Phi_b}{e} + \frac{\left(z - \frac{1}{2}\right)e}{4\pi\epsilon_0(r_0 + d)} \left(\frac{d}{\epsilon_d r_0} + \frac{1}{\epsilon_s} \right) \quad (1)$$

where Φ_b is the work function of the bulk metal, ϵ_0 , ϵ_d , and ϵ_s are the dielectric constants of the vacuum, the protecting alkanethiolate monolayer of the MPC and the medium, respectively. r_0 and d are the radius of the metallic core and the thickness of the protecting monolayer of the MPC, respectively. Figure 2b displays the potential at DPV peaks as a function of

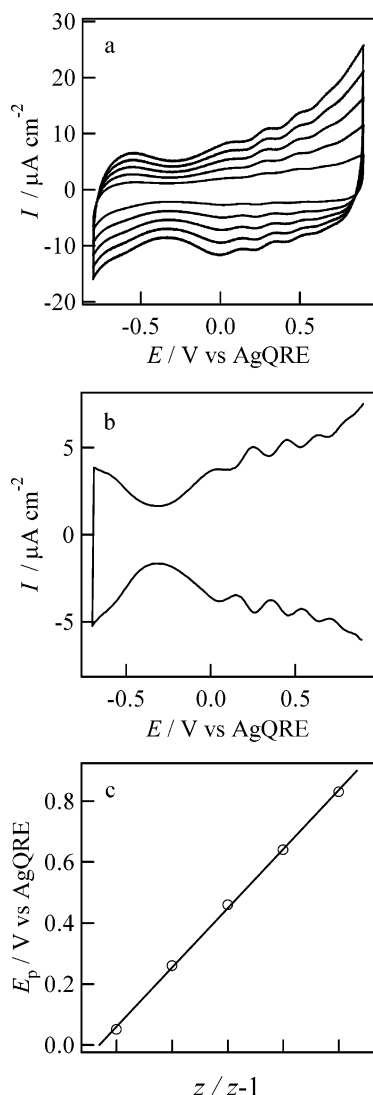


Figure 3. (a) CVs of a (C₆–C₉)Au MPC assembly in DCE at various scan rates: 0.1, 0.2, 0.3, 0.4, and 0.5 V s^{−1} from inner to outer; (b) typical DPV responses of a (C₆–C₉)Au MPC assembly in DCE; (c) linear relation between the peak potentials in (b) and the charge state of MPCs.

the MPC charge state change. The linear relation is consistent with the prediction of eq 1. In terms of eq 1, the slope of the linear fitting represents the average voltage separation of the successive redox reaction (ΔV), which is 0.25 V from the linear fitting as shown in Figure 2b. By taking $\epsilon_s = 10$ and $r_0 = d \approx 0.8$ nm, the contribution of solvent dielectric to ΔV can be evaluated to be around 0.09 V, indicating that it is a key parameter to describe the redox properties of MPCs. On the other hand, ϵ_d can also be evaluated to be 5.6. It is much larger than the intrinsic dielectric of the alkanethiolate, 3.0, while close to the value of 6.2 estimated previously,¹³ which indicates the penetration of solvent or electrolyte into the protecting monolayer of the MPCs.

As demonstrated previously, the successive electron-transfer reactions not only occur for freely diffusing MPCs in electrolyte solutions but also for MPCs in the surface assemblies. Figure 3a and b show the CVs and DPVs of a C₆Au MPC monolayer on a gold slide electrode surface linked by 1,9-nonanedithiol in DCE electrolyte solution. The responses were very consistent with those observed with the C₆Au MPCs in organic electrolyte solutions, in particular in the positive potential regime. Because the solution was not degassed, the potential scan in the negative

potential side is limited by the oxygen dissolved in the solution. On the other hand, a large potential separation between the first oxidation and the first reduction potential peaks was observed with a current minimum at around −0.30 V. The reason for this phenomenon has been considered to be due to the diffuse double layer outside the protecting monolayer,⁷ however, this effect could be worthy of dedicated studies to fully elucidate the phenomenon.

There is a linear correspondence between the oxidation peak potential and the MPC charge state, as demonstrated in Figure 3c. The linear fitting yields a slope of 0.20 V. Apparently, there is a $\sim 25\%$ decrease (from 0.25 to 0.20 V) in ΔV when MPCs are anchored onto the electrode compared to that when they are freely diffusive in the same DCE electrolyte solution. This observation is rather similar to that illustrated in a previous work, where a 25% decrease of the potential spacing took place when the particles are anchored onto the electrode surface as compared to those that are dissolved in solutions.¹⁶ The authors have considered it to be likely the preferential assembling of the larger-sized particles onto the electrode surface during the self-assembling process. However, there is neither theoretical nor experimental evidence that supports this speculation.

First of all, the partial ligand exchange of 1-hexanethiol by 1,9-nonanedithiol results in the increase of the effective thickness of the protecting monolayer, that is, the parameter d in eq 1. In this case, however, a larger ΔV is anticipated according to eq 1. Indeed, previous experimental work has also demonstrated that ΔV regularly increases with increasing the thickness of the protecting monolayer.¹⁰ For example, the voltammetric response of MPCs protected by 1-decanethiolate has a larger peak separation ($\Delta V = 0.38$) relative to that protected by 1-hexanethiolate ($\Delta V = 0.27$) in 2:1 toluene/acetonitrile mixing solution. On the other hand, because the decrease of ΔV when transferring freely diffusing MPCs onto the electrode surface was observed in the same electrolyte solution, ϵ_s can be taken to be the same and will not change ΔV . Therefore, there must be some other factors responsible for the decrease of ΔV .

The present system is analogous to a well-known model system in which a redox species, for example ferrocene, is tethered to a metal electrode at a controlled distance via a self-assembled monolayer. In this configuration, the electronic coupling between the redox species and the electrode surface is critically important in determining the kinetics and the pathway of the electron-transfer reaction. The electronic coupling factor can be expressed by a matrix element within the framework of Marcus theory. However, it is difficult to be estimated because one must consider the nuclear coordinates in the redox species and the electronic structure of the electrode. For the present system, the electronic coupling between MPCs and the gold electrode would contribute to charging work and, therefore, the solvation of the MPC. In the following, we shall estimate the electronic coupling between anchored MPCs and the gold electrode by considering the classical electrostatic model of image charges. As shown in Figure 4, an MPC with charge q is placed at a point P , which is in the solution side at a distance h from the electrode/solution interface considered as a plane. An image charge locates at a point P' , which is in the metal electrode at the same distance from the interface with charge q' . Thus, by taking this electrostatic interaction effect into account, the absolute standard redox potential of MPCs attached to an electrode surface can be derived on the basis

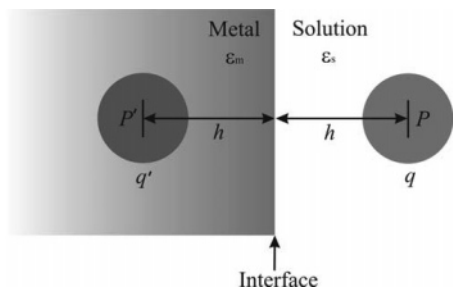


Figure 4. Application of the classical electrostatic method of image charges to an MPC self-assembled on the gold electrode surface.

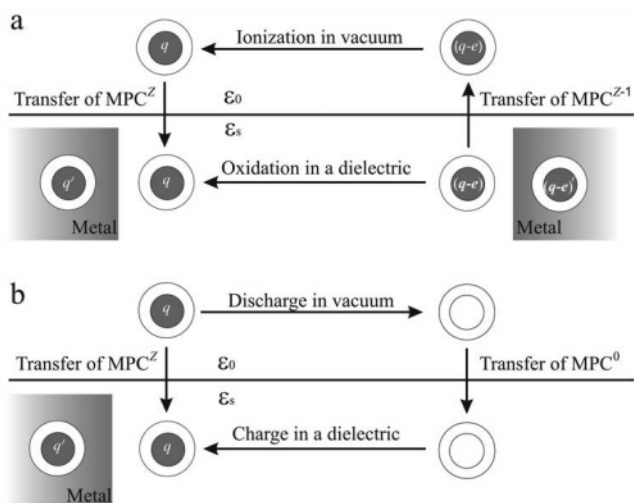


Figure 5. (a) Equivalence of an oxidation process of a surface-attached MPC to a thermodynamic cycle; (b) Born's model of the solvation of a surface-attached MPC.

of the previous work:¹³

$$[E_{ZZ-1}^0]_{\text{abs, assembly}} = [E_{ZZ-1}^0]_{\text{abs, bulk}} - \frac{(z - \frac{1}{2})e}{8\pi\epsilon_0\epsilon_s h} \quad (2)$$

In comparison with eq 1, one more term appears in eq 2. As a first approximation, this term represents the contribution from the electrostatic interaction between attached MPCs and the substrate electrode. By taking $\epsilon_s = 10$ for DCE and $h = 1.3$ nm (the approximate chain length of 1,9-nonanedithiol), a decrease of 0.06 V in ΔV is expected due to the MPC–electrode interaction. If we deduct the possible increase of ΔV for the partial ligand exchange, this value could be close to the experimentally observed 0.05 V. This conformity indicates that the electrostatic interaction between MPCs and the substrate electrode is an important factor in dictating the absolute standard redox potential of MPCs self-assembled on the electrode surface.

To derive eq 2, we consider the surface-attached MPCs as multivalent redox species and depict the sequential one-electron-transfer process as an electrochemical reaction:



As we did previously to derive eq 1,¹³ the absolute standard redox potential can be expressed by a thermodynamic cycle. As shown in Figure 5a, the one-electron oxidation reaction can be decomposed to three steps: the transfer of MPC^{Z-1} from the solvent phase to the gas phase, the ionization of MPC^{Z-1} to form MPC^Z in the gas phase, and the transfer of MPC^Z from the gas phase to the solvent phase. The difference between this

cycle and the previous one¹³ is that, in solvent phase, the electrostatic interaction will be taken into account. At a first approximation, the work to transfer a charged sphere from the gas phase to a solvent phase can be considered equal to the Gibbs solvation energy of the charged sphere. Therefore, the absolute standard redox potential, $[E_{ZZ-1}^0]_{\text{abs}}$, is given by:

$$[E_{ZZ-1}^0]_{\text{abs}} = \frac{\Delta G_{\text{solv, MPC}^Z}^0 - \Delta G_{\text{solv, MPC}^{Z-1}}^0 + E_{\text{I, Z-1}}^0}{e} \quad (4)$$

where $E_{\text{I, Z-1}}^0$ is the ionization energy of MPC^{Z-1} in a vacuum. $\Delta G_{\text{solv, MPC}^Z}^0$ and $\Delta G_{\text{solv, MPC}^{Z-1}}^0$ represent the standard Gibbs solvation energies of MPC^Z and MPC^{Z-1} , respectively.

Evaluation of $\Delta G_{\text{solv, MPC}^Z}^0$ can be done on the basis of Born's model of ionic solvation, as illustrated in Figure 5b. The work of transferring MPC^Z from the gas phase to the solvent phase ($\Delta G_{\text{solv, MPC}^Z}^0$) corresponds to the sum of the work of discharging MPC^Z in a vacuum to form a neutral sphere of the same size (w_d^0), the work of transferring this neutral sphere from the vacuum to the phase (w_n), and the work of charging this sphere in the solvent phase (w_c^s):

$$\Delta G_{\text{solv, MPC}^Z}^0 = w_d^0 + w_c^s + w_n \quad (5)$$

According to the description in Figure 5b, the electrostatic interaction between MPCs and the gold electrode only changes w_c^s , but not w_d^0 and w_n . w_d^0 has the same expression as previously derived for a freely diffusing MPC:¹³

$$w_d^0 = -\frac{z^2 e^2}{8\pi\epsilon_0} \left[\left(1 - \frac{1}{\epsilon_d}\right) \left(\frac{1}{r_0 + d}\right) + \frac{1}{\epsilon_d r_0} \right] \quad (6)$$

However, w_c^s is the sum of the work of charging a freely diffusing MPC ($w_{c,f}^s$) and the work with respect to the electrostatic interaction between anchored MPCs and the gold electrode ($w_{c,e}^s$):

$$w_c^s = w_{c,f}^s + w_{c,e}^s \quad (7)$$

where

$$w_{c,f}^s = \frac{z^2 e^2}{8\pi\epsilon_0} \left[\left(\frac{1}{\epsilon_s} - \frac{1}{\epsilon_d}\right) \left(\frac{1}{r_0 + d}\right) + \frac{1}{\epsilon_d r_0} \right] \quad (8)$$

And $w_{c,e}^s$ will be considered in terms of the classical electrostatic model of image charges. For simplicity, an MPC is considered as a large ion with an effective radius of $r_0 + d$. According to Gauss's law, the potential generated by the image charge at P is:

$$V'(q) = \frac{q'}{4\pi\epsilon_0\epsilon_s \cdot 2h} = \frac{\epsilon_s - \epsilon_m}{\epsilon_s + \epsilon_m} \cdot \frac{q}{4\pi\epsilon_0\epsilon_s \cdot 2h} \quad (9)$$

The dielectric constant of the metal electrode, ϵ_m , can be considered to be very large, and in this case, eq 9 reduces to:

$$V'(q) = -\frac{q}{4\pi\epsilon_0\epsilon_s \cdot 2h} \quad (10)$$

Then the electrostatic interaction energy induced by the image charge, $w_{c,e}^s$, can be expressed as:

$$w_{c,e}^s = \int_0^{ze} V'(q) dq = -\frac{z^2 e^2}{8\pi\epsilon_0\epsilon_s \cdot 2h} \quad (11)$$

By introducing eqs 8 and 11 to eq 7, w_c^s is obtained:

$$w_c^s = \frac{z^2 e^2}{8\pi\epsilon_0} \left[\left(\frac{1}{\epsilon_s} - \frac{1}{\epsilon_d} \right) \left(\frac{1}{r_0 + d} \right) + \frac{1}{\epsilon_d r_0} - \frac{1}{2\epsilon_s h} \right] \quad (12)$$

By substituting eqs 6 and 12 into eq 5, $\Delta G_{\text{solv, MPCZ}}^0$ is rewritten as:

$$\Delta G_{\text{solv, MPCZ}}^0 = \frac{z^2 e^2}{8\pi\epsilon_0} \left[\left(\frac{1}{\epsilon_s} - 1 \right) \left(\frac{1}{r_0 + d} \right) - \frac{1}{2\epsilon_s h} \right] + w_n \quad (13)$$

The ionization energy of MPC^{Z-1} in a vacuum ($E_{\text{I,Z-1}}^0$) is equal to the sum of the work function of the bulk metal and the work of charging an MPC from charged state $z - 1$ to z in a vacuum.^{20,21} Neither of these two works is affected by the electrostatic interaction. It means that $E_{\text{I,Z-1}}^0$ is the same for a freely diffusing and a surface-attached MPC^{Z-1} .¹³

$$E_{\text{I,Z-1}}^0 = \Phi + \frac{(2z-1)e^2}{8\pi\epsilon_0} \left[\frac{1}{\epsilon_d} \left(\frac{1}{r_0} - \frac{1}{r_0 + d} \right) + \left(\frac{1}{r_0 + d} \right) \right] \quad (14)$$

Finally, from eqs 4, 13, and 14, the absolute standard redox potential of MPCs attached to electrode surface can be derived as:

$$[E_{\text{Z/Z-1}}^0]_{\text{abs, assembly}} = \frac{\Phi_b}{e} + \frac{\left(z - \frac{1}{2} \right) e}{4\pi\epsilon_0(r_0 + d)} \left[\frac{d}{\epsilon_d r_0} + \frac{1}{\epsilon_s} - \frac{r_0 + d}{2\epsilon_s h} \right] \quad (15)$$

By combining eqs 1 and 15, we can arrive at eq 2.

Definitely, the theoretical consideration based solely on the assumption of the MPC molecular capacitance is not sufficient to describe the redox behavior of surface self-assembled MPCs.⁵ According to eq 15, there are three contributions to the absolute standard redox potential of surface self-assembled MPCs, the MPC molecular structure (this term can be related to the MPC molecular capacitance), the solvent dielectric, and the electrostatic interaction. Therefore, it is important to note that, in the present work, the influence of the electrostatic interaction on the redox properties of attached MPCs has been considered and experimentally justified. However, it should be mentioned that the redox property of MPCs is an interesting but rather complicated topic because a variety of factors that play roles in it. Indeed, an even smaller peak-to-peak spacing, for example 0.15 V, has been observed in voltammetric responses of surface self-assembled MPCs in aqueous media.¹⁶ Because ϵ_s is very large, the influence of both the solvent dielectric and the electrostatic interaction would be minor. In this case, the much smaller ΔV can be ascribed mainly to the increment of ϵ_d caused

by the penetration electrolyte ions into the protecting monolayer of the MPC, which has been found to control the electron-transfer reaction between MPCs and the substrate electrode termed as "ion rectification".¹⁶

4. Conclusions

The redox properties of alkanethiolate monolayer-protected gold nanoclusters (MPCs) self-assembled on the gold slide electrodes were studied in DCE electrolyte solutions. The effect of the electrostatic interaction between attached MPCs and the substrate electrode on the redox behavior of MPCs was theoretically considered in terms of the method of images in classical electrostatics and justified experimentally.

Acknowledgment. The work was supported by grants from the Fonds National Suisse de la Recherche Scientifique and EPFL. B.S. thanks Mr. Mohamad Hojeij for his kind help to fabricate gold slide electrodes. The technical assistance by Valérie Devaud is also acknowledged.

References and Notes

- (1) Brust, M.; Walker, M.; Bethell, D.; Schiffrin, D. J.; Whyman, R. *J. Chem. Soc., Chem. Commun.* **1994**, 801–802.
- (2) Brust, M.; Fink, J.; Bethell, D.; Schiffrin, D. J.; Kiely, C. J. *J. Chem. Soc., Chem. Commun.* **1995**, 1655–1656.
- (3) Ingram, R. S.; Hostetler, M. J.; Murray, R. W.; Schaaff, T. G.; Khoury, J.; Whetten, R. L.; Bigioni, T. P.; Guthrie, D. K.; First, P. N. *J. Am. Chem. Soc.* **1997**, *119*, 9279–9280.
- (4) Chen, S.; Ingrma, R. S.; Hostetler, M. J.; Pietron, J. J.; Murray, R. W.; Schaaff, T. G.; Khoury, J. T.; Alvarez, M. M.; Whetten, R. L. *Science* **1998**, *280*, 2098–2101.
- (5) Chen, S.; Murray, R. W.; Feldberg, S. W. *J. Phys. Chem. B* **1998**, *102*, 9898–9907.
- (6) Templeton, A. C.; Wuelfing, W. P.; Murray, R. W. *Acc. Chem. Res.* **2000**, *33*, 27–36.
- (7) Quinn, B. M.; Liljeroth, P.; Ruiz, V.; Laaksonen, T.; Kontturi, K. *J. Am. Chem. Soc.* **2003**, *125*, 6644–6645.
- (8) Chen, S. *J. Electroanal. Chem.* **2004**, *574*, 153–165.
- (9) Su, B.; Eugster, N.; Girault, H. H. *J. Am. Chem. Soc.* **2005**, *127*, 10760–10766.
- (10) Hicks, J. F.; Templeton, A. C.; Chen, S.; Sheran, K. M.; Jasti, R.; Murray, R. W.; Debord, J.; Schaaff, T. G.; Whetten, R. L. *Anal. Chem.* **1999**, *71*, 3703–3711.
- (11) Miles, D. T.; Murray, R. W. *Anal. Chem.* **2003**, *75*, 1251–1257.
- (12) Guo, R.; Georganopoulou, D.; Feldberg, S. W.; Donkers, R.; Murray, R. W. *Anal. Chem.* **2005**, *77*, 2662–2669.
- (13) Su, B.; Girault, H. H. *J. Phys. Chem. B* **2005**, *109*, 11427–11431.
- (14) Chen, S.; Murray, R. W. *J. Phys. Chem. B* **1999**, *103*, 9996–10000.
- (15) Chen, S. *J. Phys. Chem. B* **2000**, *104*, 663–667.
- (16) Chen, S.; Pei, R. *J. Am. Chem. Soc.* **2001**, *123*, 10607–10615.
- (17) Jhaveri, S. D.; Lowy, D. A.; Foos, E. E.; Snow, A. W.; Ancona, M. G.; Tender, L. M. *Chem. Commun.* **2002**, 1544–1545.
- (18) Pietron, J. J.; Hicks, J. F.; Murray, R. W. *J. Am. Chem. Soc.* **1999**, *121*, 5565–5570.
- (19) Hicks, J. F.; Zamborini, F. P.; Murray, R. W. *J. Phys. Chem. B* **2002**, *106*, 7751–7757.
- (20) Weaver, M. J.; Gao, X. *J. Phys. Chem.* **1993**, *97*, 332–338.
- (21) Makov, G.; Nitzan, A.; Brus, L. E. *J. Chem. Phys.* **1988**, *88*, 5076–5085.